Thermal Unfolding of Three Acclimation Temperature-Associated Isoforms of Carp Light Meromyosin Expressed by Recombinant DNAs†

Makoto Kakinuma,‡ Misako Nakaya, Akimasa Hatanaka, Yasushi Hirayama, and Shugo Watabe*

Laboratory of Aquatic Molecular Biology and Biotechnology, Graduate School of Agricultural and Life Sciences, The University of Tokyo, Bunkyo, Tokyo 113-8657, Japan

Kayo Maeda

International Institute for Advanced Research, Matsushita Electric Industrial Co., Ltd., Hikaridai, Seika, Kyoto 619-0237, Japan

Tatsuo Ooi

Department of Food Science, Kyoto Women's University, Higashiyama, Kyoto 605-0926, Japan

Suechika Suzuki

Department of Physiology, School of Medicine, Teikyo University, 2-11-1, Kaga, Itabashi, Tokyo 173-0003, Japan

Received September 22, 1997; Revised Manuscript Received February 27, 1998

ABSTRACT: Differential scanning calorimetry (DSC) was performed to investigate thermodynamic properties of three carp fast skeletal light meromyosin (LMM) isoforms expressed in *Escherichia coli* by recombinant DNAs. Three isoforms were the 10 °C-, intermediate-, and 30 °C-type LMM predominantly expressed in carp acclimated to 10, 20, and 30 °C. The isoforms expressed in *E. coli* by recombinant DNAs exhibited a typical pattern of α-helix in CD spectroscopy with two minima at 222 and 208 nm. Moreover, the three isoforms formed paracrystals typical of LMM, suggesting that expressed proteins retained intact structural properties. When the LMM isoforms were subjected to DSC analysis, the 10 °C and 30 °C types showed endotherms having transition temperatures (T_m) at 35.1 and 39.5 °C, respectively, which are responsible for thermal unfolding of α-helix. The intermediate type exhibited two comparable endotherms with T_m values at 34.9 and 40.6 °C, implying that it has intermediate thermodynamic properties between those of 10 °C and 30 °C types. However, a chimeric LMM having the 10 °C and 30 °C type as N- and C-terminal halves, respectively, showed the DSC pattern typical of the whole 30 °C-type molecule. On the other hand, another chimeric LMM composed of the N-terminal 30 °C type and C-terminal 10 °C type gave the pattern of the full 10 °C type. These results suggest that thermodynamic properties of the C-terminal half largely account for thermal unfolding of the whole molecule.

Sarcomeric myosins consist of two heavy chains of about 200 kDa and four light chains of about 20 kDa (*1*). Myosin heavy chain is a multidomain protein and composed of N-terminal two-globular heads, subfragment-1 (S1), and C-terminal rodlike tail that forms a coiled-coil structure of α-helices. S1 contains ATP-hydrolysis and actin-binding sites, whereas the rod domain is responsible for the assembly of myosin into thick filaments (*2*). The two fragments are easily cleaved by limited proteolysis, and the rod part is further hydrolyzed into two fragments called subfragment-2 and light meromyosin (LMM), corresponding to the N- and C-terminal halves of rod, respectively.

Differential scanning calorimetry (DSC) reveals cooperative domain structures and interactions in proteins during the progress of the unfolding reaction as well as the calorimetric heat associated with the reaction (*3*, *4*). DSC has already been proven to be useful for examining thermal unfolding of myosin and its subfragments from rabbit fast skeletal muscle (*5*−*7*). DSC was also employed to study thermal unfolding of proteins from carp acclimated to different temperatures (*8*, *9*). Differences in the thermal stability reflecting structural properties were clearly demonstrated by DSC data for myosin and its rod from carp acclimated to 10 and 30 °C. The transition temperature (T_m) of the highest endothermic peak among the three found in the 10 °C-acclimated carp proteins was about 7 °C lower than that of the highest peak in the 30 °C-acclimated carp counterparts, suggesting that the former proteins are less thermostable than the latter (*8*). Furthermore, carp LMM showed two endotherms with acclimation temperature-specific T_m values corresponding roughly to those of myosin rod, implying that thermodynamic properties of myosin rod are mainly attributable to those of LMM (*9*).

Molecular mechanisms involved in thick filament formation and assembly of sarcomeric myosins have been extensively studied, focusing on myosin rod and its C-terminal

† This study was supported in part by Grant-in-Aid for scientific research from the Ministry of Education, Science, Sports and Culture of Japan and from the Asahi Glass Foundation.

* To whom correspondence should be addressed: Tel +81-3-3812-2111, ext 7520; Fax +81-3-5684-0622; e-mail awatabe@hongo.ecc.u-tokyo.ac.jp.

‡ Present address: Laboratory of Marine Biochemistry, Department of Chemistry of Fishery Resources, Mie University, Tsu, Mie 514-8507, Japan.

S0006-2960(97)02344-1 CCC: $15.00
Published on Web 04/16/1998

half, LMM. Characteristic variation in surface hydrophobicity and charge along the length of the rod may play an important role in filament assembly and determining the stagger at which dimers associate (*10*). It had been reported that at least one region located at the N- or C-terminus of LMM is necessary for filament formation (*11*). Later, the C-terminal region of LMM was demonstrated to be essential to filament formation by using proteins from bacterial expression systems (*12*−*14*). A specific 29-residue sequence near the C-terminus of the rod, which contains a central negative charge flanked by two distinct positive blocks, appears to be required for thick filament formation (*15*). However, their precise structural interpretation is still under debate despite such extensive efforts.

Three LMM isoforms of carp fast skeletal muscle expressed in association with acclimation temperature share over 95% identity in their primary structures (*16*), although they apparently have different thermal stabilities as described before (*9*). Therefore, carp LMM isoforms seem to be a good target for investigating the relationship between the structure and thermodynamic properties that possibly affect their physiological functions such as filament formation, filament assembly, and further energy transduction from the cross-bridge head, S1, to the myosin-containing thick filament. However, LMM prepared from thermally acclimated carp consists of three LMM isoforms with different compositions. Therefore, it is difficult to identify amino acids or even regions responsible for different thermostabilities of such LMM preparations and thus to interpret structural differences in terms of thermodynamic properties.

The objective of this study was to obtain three LMM isoforms of carp fast skeletal muscle by recombinant DNAs in *Escherichia coli* and to compare their DSC and related CD patterns in order to identify which regions of the molecule are responsible for their thermodynamic properties.

MATERIALS AND METHODS

Materials. Carp cDNA clones pMHC10-3, pMHC10-25, and pMHC30-6, encoding the 10 °C-, intermediate-, and 30 °C-type LMMs, respectively (*16*), were used to construct recombinant DNAs with pET-11a and *E. coli* BL21(DE3)-pLysS (Novagene) as an expression vector and host bacterium, respectively. All reagents used in this study were of analytical grade.

Construction of Carp Light Meromyosin Expression Vectors. Expression vectors pET10, pET I, and pET30, containing DNA fragments encoding carp 10 °C-, intermediate-, and 30 °C-type LMMs, respectively, were constructed as follows. The relevant plasmid pET-11a expression vector contained *Nhe*I and *Bam*HI sites in a multiple cloning site. The fragments for inserts encoding carp LMMs were amplified by PCR (*17*) using pMHC10-3, pMHC10-25, and pMHC30-6 as templates, together with primers P-10T (5′-GAGGTGGCCGCTAGCAGAGCCAAATATGAGACTGATGC-3′) and P-10E (5′-AGTTTCGGATCCTCATTCTTCAACTTTAGTCTTCCC-3′), primers P-10T and P-IE (5′-TTCTTGGGATCCTTATTCATCTTTAGTCTTTCCAGC-3′), and primers P-30T (5′-GAGGTGGCTGCTAGCAGAACCAAATATGAGACTGATGCC-3′) and P-30E (5′-GATGGCGGATCCTCATTCTTCATCCTTGCTCTTCCC-3′) containing *Nhe*I and *Bam*HI recognition sites, respectively. The PCR products were digested with *Nhe*I and *Bam*HI and subcloned into a *Nhe*I-*Bam*HI site of pET-11a. After the sequences of the inserted DNA fragments were confirmed, expression vectors pET10, pETI, and pET30 constructed from pMHC10-3, pMHC10-25, and pMHC30-6, respectively, were transformed into *E. coli* strain BL21(DE3)pLysS in which expression was controlled by the *lacI* repressor.

Expression vector pET10N-30C contained a chimeric DNA fragment encoding the N-terminal half of the 10 °C type and the C-terminal half of the 30 °C type, whereas pET30N-10C consisted of a fragment encoding the N-terminal half of the 30 °C type and the C-terminal half of the 10 °C type. Chimeric LMM expression vectors were constructed using a unique restriction site (*Nco*I site) within DNA fragments encoding both LMMs. Two fragments of about 800 bp encoding C-terminal halves of the 10 °C- and 30 °C-type LMMs were obtained from pET10 and pET30 by *Nco*I-*Bam*HI digestion. These fragments were subcloned into the *Nco*I-*Bam*HI sites of pET30 and pET10, respectively.

Bacterial Expression and Protein Purification. Carp 10 °C-, intermediate-, and 30 °C-type LMMs expressed in *E. coli* were purified essentially as described by Maeda et al. (*18*) and Watabe et al. (*19*). Overnight cultures (40 mL) of *E. coli* containing expression vectors pET10, pETI, and pET30 were inoculated into 1.6 L of LB medium and grown at 20 °C for pET10 and pETI and at 30 °C for pET30. When the cultures reached an absorbance of 0.5 at 600 nm, expression of the proteins was induced by the addition of isopropyl β-D-thiogalactopyranoside (IPTG) to a final concentration of 1 mM. The cultures were then grown for a further 2 h.

Cells grown were harvested by centrifugation at 3000*g* for 10 min. The pellet was washed with ice-cold 50 mM Tris-HCl (pH 7.5) and resuspended in approximately 10 volumes of ice-cold 50 mM Tris-HCl (pH 7.5) containing 0.6 M KCl, 0.5 mM dithiothreitol (DTT), 1 mM EDTA, 1 mg/mL freshly dissolved lysozyme, 0.1 mM phenylmethanesulfonyl fluoride, 0.5 μg/mL pepstatin A, 0.5 μg/mL leupeptin, and 0.5 μg/mL E-64. After incubation at 4 °C for 2 h, cells were sonicated with a Tomy UD-201 ultrasonic disrupter. The lysates were centrifuged at 35000*g* for 60 min, and the resulting supernatant was dialyzed against 10 mM potassium phosphate (pH 7.5) containing 0.1 M KCl and 0.5 mM DTT. After dialysis, the precipitate obtained by centrifugation at 100000*g* for 60 min was dissolved in and dialyzed against 10 mM potassium phosphate (pH 7.5) containing 0.6 M KCl and 0.5 mM DTT and centrifuged at 100000*g* for 60 min. The supernatant was dialyzed once more against 10 mM potassium phosphate (pH 7.5) containing 0.1 M KCl and 0.5 mM DTT, and centrifuged at 100000*g* for 60 min. The resulting precipitate was dissolved in 20 mM sodium pyrophosphate (pH 7.5) containing 30 mM KCl, 1 mM DTT, and 1 mM EDTA. After dialysis, the solution was applied to a DEAE-Toyopearl 650M ion-exchange column (1.4 × 26 cm) equilibrated with the same buffer, whereas proteins adsorbed were eluted with a linear gradient from 30 to 600 mM KCl. Fractions containing the 10 °C-, intermediate-, and 30 °C-type LMMs were concentrated by ultrafiltration.

Protein concentrations were determined by the biuret method of Gornall et al. (*20*) using bovine serum albumin (BSA) as the standard.

Sodium Dodecyl Sulfate−Polyacrylamide Gel Electrophoresis. Sodium dodecyl sulfate−polyacrylamide gel electrophoresis (SDS−PAGE) was carried out by the method of Laemmli (*21*), using 12.5% polyacrylamide slab gels containing 0.1% SDS. Gels were stained with Coomassie Brilliant Blue (CBB) R-250 and destained with a solution containing 25% methanol and 7% acetic acid.

Concentrations of purified LMMs in CBB-stained SDS−PAGE gels were estimated by measuring the absorbance of the protein band at 565 nm with a Shimadzu dual-wavelength flying spot scanning densitometer, model CS-9300PC, coordinated with a QuantaScan 2D software.

N-Terminal amino acid sequences were determined essentially as described by Matsudaira (*22*). Proteins in SDS−polyacrylamide gels were electroblotted to poly(vinylidene difluoride) (PVDF) membranes. Protein bands visualized by staining with CBB were cut and put onto a Blott cartridge block and analyzed for sequences with a Perkin-Elmer Applied Biosystems model 476A protein sequencer.

Electron Microscopy. Paracrystal formation and negative staining were performed essentially as described by Bennet (*23*) and Yagi and Offer (*24*). For observation of paracrystals, purified LMMs at a concentration of 1 mg/mL were first dialyzed at 4 °C against 10 mM potassium phosphate (pH 7.0) containing 0.35 M KCl, and then the KCl concentration of the dialysate was lowered by 0.05 M every day to a final concentration of 0.10 M.

Negative staining was carried out with samples deposited onto carbon collodion-coated 400-mesh grids for 10−20 s. After removal of excess sample solution with a filter paper, grids were stained with 2% (w/v) uranyl acetate and dried. Negatively stained samples were observed with a JEOL 2000FXS electron microscope.

Differential Scanning Calorimetry and CD Spectrometry. DSC was carried out using a MicroCal model MC2 differential scanning microcalorimeter essentially according to Nakaya et al. (*8*). The solvent used was 50 mM Tris-HCl (pH 8.0) containing 0.6 M KCl, 5 mM $MgCl_2$, and 1 mM DTT. DSC scans were performed at a rate of 45 °C/h in a temperature range from 4 to 60 °C. Protein concentrations were in the range from 1.2 to 1.7 mg/mL. DSC data were analyzed using a software package, Origin, developed by MicroCal. An approximate subunit molecular weight of LMM used for data analysis, 65 000, was calculated from amino acid sequences (*16*, *19*). The heat capacity data were fit by using nonlinear least-squares, initially assuming that $\Delta H_{cal}/\Delta H_{vh} = 1$ where ΔH_{cal} and ΔH_{vh} are calorimetric and van't Hoff enthalpy, respectively. When the data were not fitting satisfactorily, heat capacity curves were subsequently fit by allowing ΔH_{cal} and ΔH_{vh} to float. After minimization by appropriate computer programs, the values for the thermal transition, including T_m, ΔH_{cal}, ΔH_{vh}, and molar excess heat capacity (DC_p), were obtained.

CD spectra were measured at various temperatures ranging from 4 to 60 °C in the same buffer used for DSC runs with a Jasco J-720W spectropolarimeter. A jacketed cell of 0.2 mm optical path length was used and temperature was controlled by circulating thermoregulated water. The wavelength and protein concentrations for measurement were in the ranges from 240 to 195 nm and from 1.2 to 1.7 mg/mL, respectively.

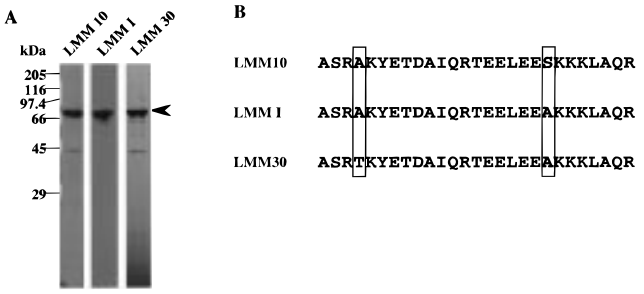

FIGURE 1: SDS−PAGE patterns and N-terminal amino acid sequences of the three carp light meromyosin isoforms expressed by recombinant DNAs. SDS−PAGE was carried out with 12.5% gels and 5 μg of sample for each lane (A). Coomassie blue-stained polyacrylamide gel of the 10 °C (LMM10), intermediate- (LMM I), and 30 °C (LMM30) type LMM isoforms expressed by and purified from *E. coli* are shown together with their N-terminal amino acid sequences (B). Boxes in amino acid sequences indicate amino acid substitutions among the three isoforms.

RESULTS

Bacterial Expression of Carp 10 °C-, Intermediate-, and 30 °C-type Light Meromyosins. Expression vectors pET10, pETI, and pET30 were constructed in pET-11a from cDNA clones, pMHC10-3, pMHC10-25, and pMHC30-6, encoding carp 10 °C-, intermediate-, and 30 °C-type LMMs, respectively (*16*). The expressed 10 °C-, intermediate-, and 30 °C-type LMM isoforms were successfully purified to homogeneity (Figure 1A). The yield of the three purified isoforms was approximately 10% of the total bacterial proteins from the cell lysate based on densitometric analysis.

The inserted DNA fragments for the 10 °C and 30 °C types contained 1689 bp encoding 563 amino acid residues, whereas the fragment for the intermediate type of 1686 bp encodes 562 amino acids. For insertion into the expression vector, an *Nhe*I recognition site was added to the 5′ end of the fragment. Therefore, isoforms expressed in *E. coli* theoretically contain two more amino acid residues, alanine and serine, at the N-terminus (Figure 1B). N-Terminal formylmethionine is supposed to be removed when proteins are expressed in this vector system (*25*, *26*). Although the molecular weights of expressed 10 °C-, intermediate-, and 30 °C-type LMM isoforms are thus expected to be 64 922, 64 821, and 65 012, respectively, these were estimated to be about 74 000 in SDS−PAGE (Figure 1A). Such differences between observed and theoretical values have been reported for rabbit fast skeletal muscle LMM (*18*, *27*) and for myosin rod of *Dictyosterium discoideum* expressed in *E. coli* (*28*). Nevertheless, an apparent molecular mass of 74 kDa in our expressed LMMs were still larger than those of the major 66 and 69 kDa components prepared from thermally acclimated carp (*9*, *19*). The two limited proteolytic digestions during preparation processes for LMM from carp muscle might give rise to cleavage of a C-terminal region of the intact LMM molecule.

CD Spectrometry for Three Carp Light Meromyosin Isoforms Expressed by Recombinant DNAs. Three carp LMM isoforms expressed by recombinant DNAs were subjected to CD spectrometry. When measured at about 20 °C, all LMMs exhibited typical patterns of α-helix having two minima at 222 and 208 nm (Figure 2). Assuming that 100% α-helical content corresponds to a value of 36 000 deg cm^{-2} $dmol^{-1}$ of [θ] at 222 nm (*29*), both the 10 °C- and

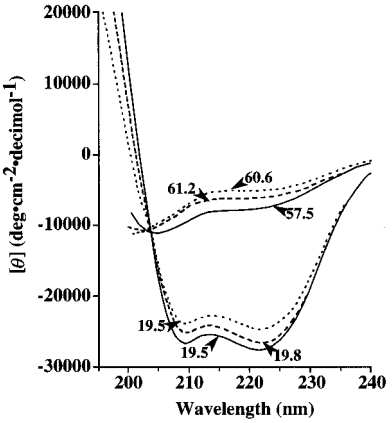

FIGURE 2: CD spectra of the three carp light meromyosin isoforms expressed by recombinant DNAs. LMM isoforms were expressed by recombinant DNAs that encode the 10 °C- (solid line), intermediate- (dotted line), and 30 °C- (dashed line) types. CD spectrometry was performed in 50 mM Tris-HCl (pH 8.0) containing 0.6 M KCl, 5 mM $MgCl_2$, and 1 mM DTT. [θ] represents the mean residue ellipticity. Protein concentrations were from 1.2 to 1.7 mg/mL, and measurement temperatures are indicated.

30 °C-type LMM isoforms were calculated to have an apparent α-helical content of about 80%, whereas that of the intermediate-type isoform was about 70%, a slightly lower value than those of the other LMMs.

When temperature for measurement was increased, the values of [θ] at 222 nm for the three LMMs increased concomitantly, suggesting a temperature-dependent unfolding of α-helix. No minimum was observed at 222 nm over 50 °C. Once treated at about 60 °C and subsequently cooled to about 20 °C, the 10 °C- and 30 °C-type isoforms showed again a typical pattern of α-helix, yielding about 70% α-helical contents. On the other hand, the intermediate type showed 65% α-helical content after such treatment. Details of α-helical contents at various measuring temperatures will be described later.

Electron Microscopy of Three Carp Light Meromyosin Isoforms Expressed by Recombinant DNAs. LMM forms paracrystals at low salt concentrations, showing characteristic striations in electron microscopy after negative staining (*23*, *24*). LMM paracrystals prepared from carp acclimated to 10 and 30 °C also had a spindle-shape and often tended to be clumped together, showing tactoids that had characteristic repeating patterns of light and dark stripes perpendicular to the long axis of the paracrystal (data not shown).

Electron microscopic observations were also performed with the three LMM isoforms expressed by recombinant DNAs (Figure 3). These paracrystals exhibited a marked transverse periodicity of about 40 nm, as those prepared from thermally acclimated carp and those previously reported for other LMMs (*23*, *30*, *31*). Taken together with the results of CD spectrometry, the three LMM isoforms expressed by recombinant DNAs were regarded to have the same structures of α-helices as those from intact muscles.

Differential Scanning Calorimetry for Three Carp Light Meromyosin Isoforms Expressed by Recombinant DNAs. It was previously demonstrated that LMMs prepared from fast skeletal muscles of carp acclimated to 10 and 30 °C exhibited predominant endotherms at 32.5 and 39.5 °C, respectively, in DSC (*9*).

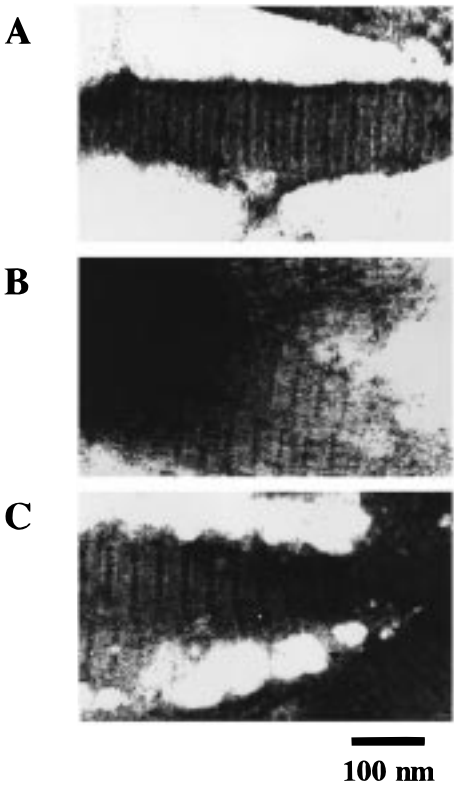

FIGURE 3: Electron micrographs for paracrystals of the three carp light meromyosin isoforms expressed by recombinant DNAs. Electron micrographs were observed with negatively stained paracrystals of the 10 °C- (A), intermediate- (B), and 30 °C- (C) type LMM isoforms expressed by *E. coli*. LMMs in 50 mM Tris-HCl (pH 8.0) containing 0.6 M KCl, 5 mM $MgCl_2$, and 1 mM DTT were first dialyzed against 10 mM potassium phosphate (pH 7.0) containing 0.3 M KCl, and then the KCl concentration of the dialysate was lowered to give a final concentration of 0.1 M. The bar represents 100 nm.

In the present study, two prominent endotherms, one major and the other minor, having T_m at 35.1 and 53.4 °C were found in the 10 °C-type LMM with ΔH_{cal} of 114.2 and 20.7 kcal/mol, respectively (Figure 4A and Table 1). On the other hand, one large peak was found at about 40 °C in the 30 °C-type LMM. However, the deconvolution analysis for the 30 °C type gave two endotherms having T_m at 35.4 and 39.5 °C with ΔH_{cal} of 87.3 and 59.0 kcal/mol, respectively (Figure 4C and Table 1).

The intermediate-type LMM showed two prominent endotherms having T_m at 34.9 and 40.6 °C. The deconvolution analysis gave three endotherms with T_m at 34.9, 40.6, and 44.9 °C with ΔH_{cal} of 29.3, 40.1, and 2.7 kcal/mol, respectively (Figure 4B and Table 1). It was noted that the two T_m values at 34.9 and 40.6 °C for the major endotherms found in the intermediate-type were comparable to those at 35.1 and 39.5 °C of the highest peaks for the 10 °C- and 30 °C-type LMMs, respectively. Although the endotherms with T_m at about 35 and 40 °C were also obtained with the 30 °C type, DSC patterns were apparently different between the intermediate- and 30 °C-type isoforms.

Temperature-Dependent Changes in CD Spectra for Three Carp Light Meromyosin Isoforms Expressed by Recombinant DNAs. α-Helical contents were determined by CD spectrometry at various temperatures for LMMs expressed by recombinant DNAs. Plots of α-helical content against measuring temperatures for the three LMM isoforms are

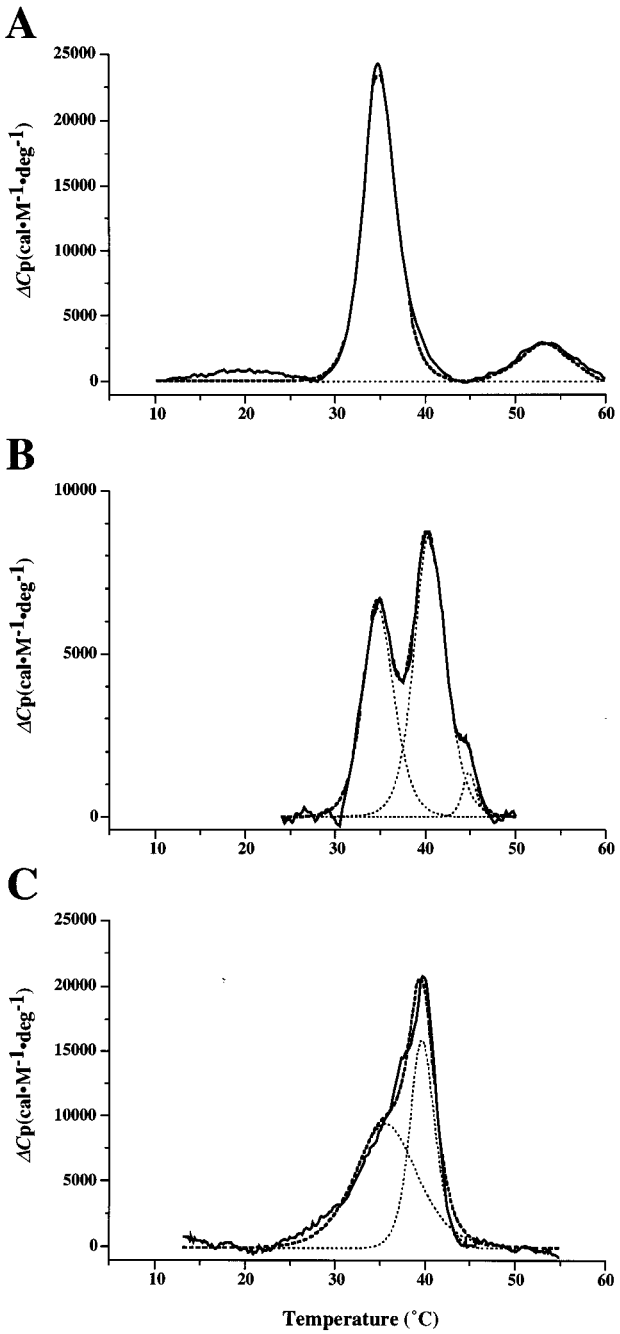

FIGURE 4: DSC scans of the three carp light meromyosin isoforms expressed by recombinant DNAs, together with their computer-calculated differential endotherms by the convolution analysis. The 10 °C- (A), intermediate- (B), and 30 °C-type (C) LMM isoforms in 50 mM Tris-HCl (pH 8.0) containing 0.6 M KCl, 5 mM $MgCl_2$, and 1 mM DTT were measured at protein concentrations of 1.61, 1.20, and 1.23 mg/mL, respectively. The observed DSC patterns (solid lines) were subjected to smoothing treatment (boldface dashed lines) and further to the convolution analysis (dotted lines) for differential endotherms. The scan rate was 45 °C/h, and data were collected every 15 s. ΔC_p represents molar excess heat capacity.

shown in Figure 5. The maximum values of the decreasing rate derivatives were observed at about 35 and 40 °C for the 10 °C- and 30 °C-type LMMs, respectively. On the other hand, the intermediate type showed two maxima at about 35 and 40 °C, each corresponding well to those of the 10° C and 30° C type, respectively. These temperatures were roughly consistent with T_m values of the main peaks in DSC analysis (Table 1). These results suggest that endotherms

Table 1: Thermodynamic Parameters on Thermal Unfolding of Carp 10 °C-, Intermediate-, and 30 °C-type Light Meromyosin Isoforms Expressed by Recombinant DNAs, Together with Those of Two Carp Chimeric Light Meromyosins

light meromyosin	T_m (°C)	ΔH_{cal} (kcal/mol)
10 °C-type[a]	35.1	114.2 (1.4)[b]
	53.4	20.7 (5.6)
intermediate-type[c]	34.9	29.3 (5.6)
	40.6	40.1 (4.2)
	44.9	2.7 (150)
30 °C-type[d]	35.4	87.3 (0.9)
	39.5	59.0 (3.6)
10N-30C chimera[e]	36.4	68.3 (1.3)
	39.5	95.9 (2.7)
30N-10C chimera[f]	35.0	93.0 (1.7)
	38.8	21.2 (7.8)

[a] Values obtained from Figure 4A. [b] Values in parentheses are ratios of ΔH_{vh} to ΔH_{cal}. [c] Values obtained from Figure 4B. [d] Values obtained from Figure 4C. [e] LMM composed of the N-terminal half of the 10 °C type and the C-terminal half of the 30 °C type. Values were obtained from Figure 7A. [f] LMM composed of the N-terminal half of the 30 °C type and the C-terminal half of the 10 °C type. Values were obtained from Figure 7B.

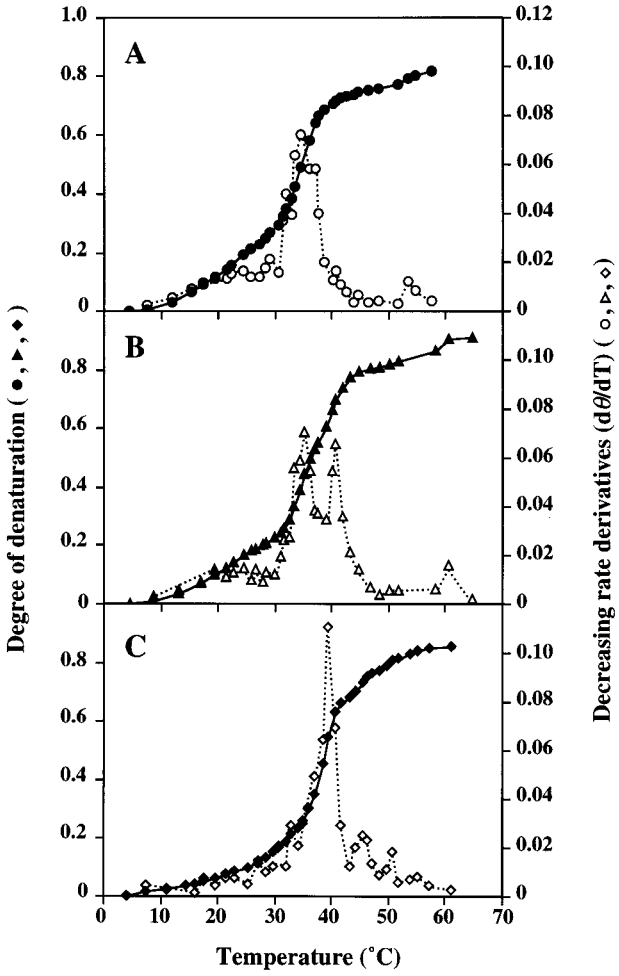

FIGURE 5: Decreasing rate derivatives of the mean residue ellipticity against temperatures for the three carp light meromyosin isoforms expressed by recombinant DNAs. Data show the degree of denaturation against temperatures and decreasing rate derivatives of the mean residue ellipticity, $[\theta]$, of the 10 °C- (A), intermediate- (B), and 30 °C-type (C) LMM isoforms expressed by *E. coli*. The decreasing rate derivatives ($d[\theta]/dT$) (open symbols) were calculated from the increment of $[\theta]$ at 222 nm (degree of denaturation, closed symbols) per unit change of temperature.

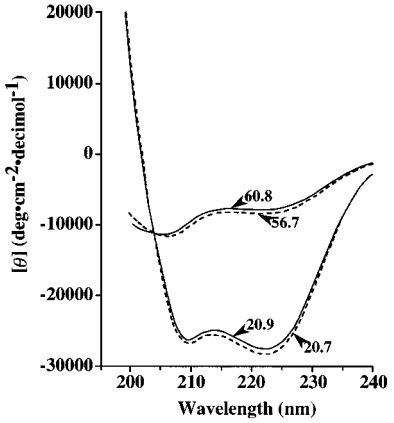

FIGURE 6: CD spectra of chimeric carp light meromyosins expressed by recombinant DNAs. Chimeric LMMs contained the N-terminal half of the 10 °C type and the C-terminal half of the 30 °C type (10N-30C) (solid lines) and *vice versa* (30N-10C) (dashed lines). The protein concentration was 1.67 mg/mL, and measurement temperatures are indicated. Refer to the caption of Figure 2 for other experimental conditions.

of LMM mainly result from unfolding of α-helix, as observed with LMMs from the 10 °C- and 30 °C-acclimated carp (*9*). It was again clearly demonstrated that the intermediate type has an intermediate feature between those of the 10 °C- and 30 °C types. Since unfolding of α-helix was hardly observed at about 35 °C with the 30 °C type, a large endotherm at this temperature in DSC run for the 30 °C type (see Figure 5C) would be caused by other factor(s) including, for example, melting of coiled-coil structure.

CD Spectrometry for Two Chimeric Light Meromyosins Expressed by Recombinant DNAs. Two chimeric LMM expression vectors, pET10N-30C and 30N-10C, were constructed. The pET10N-30C expressed LMM consisting of the N-terminal half of the 10 °C type and the C-terminal half of the 30 °C type, whereas the pET30N-10C expressed LMM composed of the opposite halves. Chimeric LMMs expressed by these recombinant DNAs in *E. coli* were purified to homogeneity, and their molecular weights were estimated to be about 74 000, the same as those of three carp LMM isoforms in SDS−PAGE (data not shown).

Then the two chimeric LMMs, 10N-30C and 30N-10C, were subjected to CD analysis. Both chimeric LMMs exhibited typical patterns of α-helix as shown in Figure 6, exhibiting two minima at 222 and 208 nm, the same as those of the three types of carp LMMs expressed by *E. coli*. Apparent α-helical contents were calculated to be about 85% at about 20 °C for the two chimeric LMMs. They lost most α-helical structure at about 60 °C. However, such LMMs once heated at about 60 °C restored about 70% α-helix when measured again at about 20 °C.

Moreover, they formed the same paracrystals (data not shown) as observed for LMMs from thermally acclimated carp and those expressed by recombinant DNAs. These results suggest that the two chimeric LMMs have the same structures as those of native LMMs prepared from intact muscles.

Differential Scanning Calorimetry and Temperature-Dependent Changes in CD Spectra for Two Chimeric Light Meromyosins Expressed by Recombinant DNAs. In DSC analysis, a major peak was observed at about 40 °C with the 10N-30C chimeric LMM and at about 35 °C with the

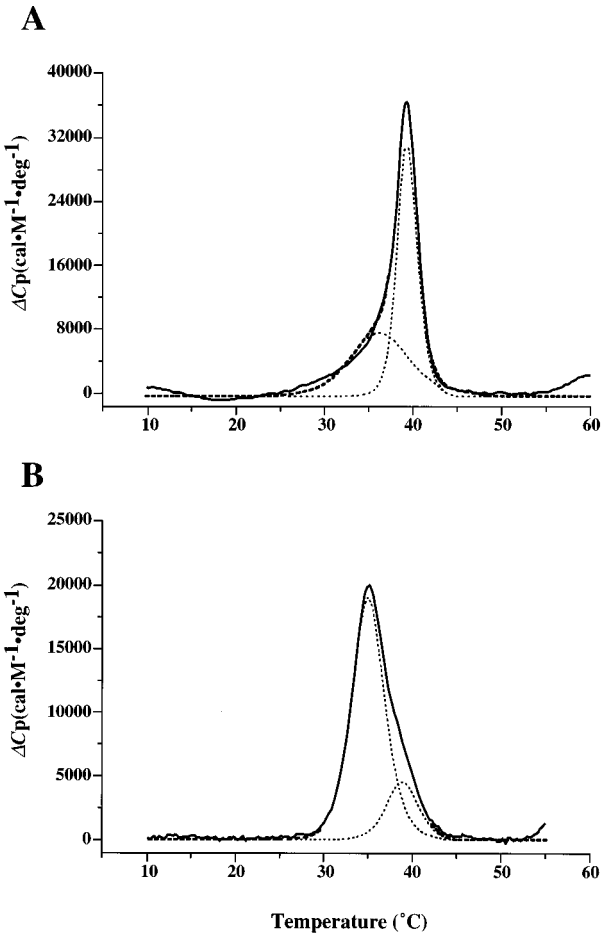

FIGURE 7: DSC scans of chimeric carp light meromyosins together with their computer-calculated differential endotherms by the convolution analysis. Chimeric LMM contained the N-terminal half of the 10 °C-type and the C-terminal half of the 30 °C-type (10N-30C) (A) and *vice versa* (30N-10C) (B). The protein concentration was 1.67 mg/mL. Refer to the caption of Figure 4 for other experimental conditions.

30N-10C LMM (Figure 7). The deconvolution analysis for the 10N-30C LMM showed two endotherms having T_m at 36.4 and 39.5 °C with ΔH_{cal} of 68.3 and 95.9 kcal/mol, respectively, whereas the 30N-10C LMM gave two endotherms having T_m at 35.0 and 38.8 °C with ΔH_{cal} of 93.0 and 21.2 kcal/mol, respectively (Table 1). Although these two T_m values were found in all the three LMM isoforms, overall DSC patterns of the 10N-30C and 30N-10C LMMs resembled those of the 30 °C and 10 °C types, respectively, differing from that of the intermediate type. Therefore, the C-terminal half of LMM seems to be mostly responsible for thermodynamic properties of the whole LMM molecule.

Plots of α-helical contents against measuring temperatures of the two chimeric LMMs are shown in Figure 8. The maximum values of the decreasing rate derivatives for the 10N-30C and 30N-10C LMM were obtained at about 40 and 35 °C, respectively, which correspond well to those of the 30 °C and 10 °C types, respectively (Table 1). Therefore, thermal unfolding of the chimeric LMM molecules appears to be dependent on the structure of the C-terminal half as revealed by comparison of DSC patterns (see Figures 4 and 7).

DISCUSSION

Different types of fast skeletal LMM are expressed in association with temperature acclimation of carp (*16*, *19*, *32*).

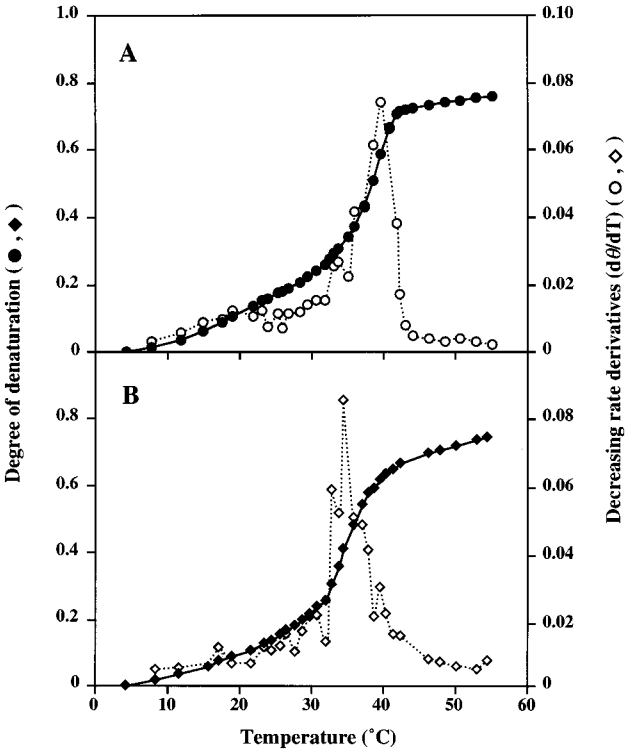

FIGURE 8: Decreasing rate derivatives of the mean residue ellipticity against temperatures for chimeric carp light meromyosins. Data show the degree of denaturation against temperatures and the decreasing rate derivatives of the mean residue ellipticity, [θ], of the 10N-30C (A) and 30N-10C (B) LMMs. Refer to the caption of Figure 7 for the chimeric LMMs, and to that of Figure 5 for the degree of denaturation (closed symbols) and decreasing rate derivatives (open symbols).

Differences between the cold- and warm-acclimated carp LMM prevailed in the primary structure, suggesting a functional significance of the changed regions of the LMM molecule in the regulation of energy transduction from S1 to thick filaments.

Nakaya et al. (*9*) prepared LMMs from the 10 °C- and 30 °C-acclimated carp and subjected these to DSC runs. It is quite reasonable to consider that these preparations contain multiple components of LMM isoforms, changing their composition in a linear gradient of environmental temperatures from cold to warm water. Differences in the thermal stability reflecting structural properties were clearly demonstrated by DSC data for the two LMM preparations from thermally acclimated carp, suggesting that these preparations consisted predominantly of respective acclimation temperature-specific isoforms, together with minor components (*9*). To confirm such LMM isoform-specific differences in thermodynamic properties, we attempted to obtain the three isoforms, the 10 °C, intermediate, and 30 °C types, by using recombinant DNAs, the parent cDNAs of which had been previously isolated from carp (*16*).

When subjected to CD spectrometry, the three carp LMM isoforms expressed by recombinant DNAs showed α-helical contents of 70−80%. These values were slightly lower than those previously reported for LMMs prepared from carp acclimated to 10 °C and 30 °C, which were calculated to be about 90% (*9*). It has been reported that rabbit skeletal LMM contained 90% α-helix (*2*), whereas that expressed by recombinant DNA showed slightly a lower value of 70−80% (*18*).

Proteins having coiled-coil structures such as tropomyosin, paramyosin, and LMM form paracrystals, showing tactoids that have characteristic repeating patterns of light and dark stripes (*30*, *33*, *34*). Thus, electron microscopic observations on paracrystals suggest that the three carp LMM isoforms expressed by recombinant DNAs had intact coiled-coil structures of α-helices. In addition, the ratios of $\Delta H_{vh}/\Delta H_{cal}$ shown in Table 1, which reflect the number of molecules in a cooperative unit in thermal transition, are in the range of 1.4−3.6 for the major endotherms. This would also be indicative of the formation of such an assembly as a coiled-coil structure. At present, however, it is difficult to directly identify whether the expressed LMMs have the same coiled-coil structures as an intact LMM from muscle.

It has been reported that two prominent endotherms having T_m at 32.5 and 39.5 °C with ΔH_{cal} of 269 and 52 kcal/mol, respectively, were found in the 10 °C-acclimated carp LMM (*9*). It is likely that the maximum endotherm with T_m at 32.5 °C for LMM from the 10 °C-acclimated carp corresponds to that of the 10 °C-type LMM, 35.1 °C, in the present study. This difference might be caused by the lack of a C-terminal peptide in LMM preparation from intact muscle as revealed by SDS−PAGE. The endotherm with T_m at 39.5 °C for the 30 °C-type LMM was comparable to that at 39.2 °C for LMM from the 30 °C-acclimated carp (*9*). The two prominent endotherms with T_m at 34.9 and 40.6 °C for the intermediate-type LMM in the present study well agreed with those at 34.5 and 40.2 °C observed in the 20 °C-acclimated carp LMM (*9*). A minor endotherm having T_m at 53.4 °C was observed together with a major endotherm of 35.1 °C in the 10 °C-type LMM expressed by recombinant DNA (see Figure 4A and Table 1). Such high T_m value of 53.4 °C was not observed with other LMMs and cannot be reasonably explained at present. It is surprising to observe marked differences in thermodynamic properties between the 10 °C- and 30 °C-type LMM isoforms, since the two types show 95.6% identity in the primary structure (*16*).

Hwang et al. (*40*) reported that myosin Ca^{2+}-ATPase was less thermostable in the 10 °C- than the 30 °C-acclimated carp. Moreover, it has been demonstrated in in vitro motility assays that activation energy for F-actin sliding on a sheet covered with myosin from the 10 °C-acclimated carp is lower than on that covered with myosin from the 30 °C-acclimated carp (*35*). In the present study, DSC analysis demonstrated that the 30 °C-type LMM is more thermostable than the 10 °C-type LMM. Therefore, lower thermostability of the 10 °C-type LMM predominantly expressed in cold-acclimated carp is probably more suitable for energy transduction from S1 to thick filaments in low temperature, facilitating muscle movement in the cold-acclimated carp more easily.

In myosin rod, a coiled-coil structure is formed by two α-helices. The amino acid sequences that adopt the coiled-coil structure display a characteristic seven-residue repeat pattern, designated a−g, where residues a and d form the core of the coiled coil, an internal hydrophobic seam, and e and g often contain charged residues arranged so as to form salt bridges between the helices of the two monomers (*36*−*38*). Such ionic interaction is considered to strengthen the coiled-coil structure, as well as to dictate a parallel association of the two monomers. Coat positions b, c, and f are highly charged, and are exposed on the exterior of the rod, where they may mediate dimer−dimer interactions during

assembly of the higher order structure of thick filaments (*10*).

The DSC data for two chimeric LMMs indicate that thermodynamic properties of carp LMM isoforms are mainly determined by a C-terminal half of the LMM molecule. For example, the 10N-30C LMM containing the N-terminal half of the 10 °C type and the C-terminal half of the 30 °C type showed a major endotherm with T_m at 39.5 °C where the 30 °C type exhibited the largest peak on the DSC run and the maximum thermal unfolding of α-helix on CD analysis (see Figure 7). Comparison of amino acid sequences deduced from cDNA clones for the 10 °C- and 30 °C-type LMMs showed 24 amino acid substitutions, a half of which are irregularly located in the C-terminal half (*16*). Substitutions are considerably concentrated near the C-terminal end, three residues being contained within a nonhelical C-terminal region (*16*). The 535th alanine at position d in the 30 °C-type LMM is more hydrophobic than serine in the 10 °C type at the same position. Substitutions of the hydrophobic residues at positions a and d for less hydrophobic ones decrease the stability of the coiled-coil structure of α-helices (*39*). The interaction between the 536th histidine at position e and the 538th arginine at position g seems to be harmful to thermostability for the 10 °C-type LMM according to McLachlan and Stewart (*36*). Therefore, it seems that the differences in thermodynamic properties between the 10 °C- and 30 °C-type LMM isoforms are determined by such amino acid substitutions. Site-directed mutagenesis is currently being carried out along these lines.

ACKNOWLEDGMENT

We thank Shigeru Iwashita for excellent technical assistance in electron microscopy.

REFERENCES

1. Harrington, W. F., and Rodgers, M. E. (1984) *Annu. Rev. Biochem. 53*, 35−37.
2. Lowey, S., Slayter, H. S., Weeds, A. G., and Baker, H. (1969) *J. Mol. Biol. 42*, 1−29.
3. Privalov, P. L. (1979) *Adv. Protein Chem. 33*, 167−241.
4. Privalov, P. L., and Gill, S. L. (1988) *Adv. Protein Chem. 39*, 191−234.
5. Bertazzon, A., and Tsong, T. Y. (1990) *Biochemistry 29*, 6453−6459.
6. Shriver, J. W., and Kamath, U. (1990) *Biochemistry 29*, 2556−2564.
7. Swenson, C. A., and Ritchie, P. A. (1980) *Biochemistry 19*, 5371−5375.
8. Nakaya, M., Watabe, S., and Ooi, T. (1995) *Biochemistry 34*, 3114−3120.
9. Nakaya, M., Kakinuma, M., Watabe, S., and Ooi, T. (1997) *Biochemistry 36*, 9179−9184.
10. Hoppe, P. E., and Waterson, R. H. (1996) *J. Cell Biol. 135*, 371−382.
11. Akutagawa, T., and Ooi, T. (1982) *J. Biochem. (Tokyo) 92*, 999−1007.
12. Maeda, K., Rösch, A., Maeda, Y., Kalbitzer, H. R., and Wittinghofer, A. (1991) *FEBS Lett. 281*, 23−26.
13. Atkinson, S. J., and Stewart, M. (1992) *J. Mol. Biol. 226*, 7−13.
14. Hodge, T. P., Cross, R., and Kendrick-Jones, J. (1992) *J. Cell Biol. 118*, 1085−1095.
15. Sohn, R. L., Vikstrom, K. L., Strauss, M., Cohen, C., Szent-Györgyi, A. G., and Leinwand, L. A. (1997) *J. Mol. Biol. 266*, 317−330.
16. Imai, J., Hirayama, Y., Kikuchi, K., Kakinuma, M., and Watabe, S. (1997) *J. Exp. Biol. 200*, 27−34.
17. Saiki, R. K., Gelfand, D. H., Stoffel, S., Scharf, S. J., Higuchi, R., Horn, G. T., Mullis, K. B., and Erlich, H. A. (1988) *Science 239*, 487−491.
18. Maeda, K., Sczakiel, G., Hofmann, W., Menetret, J.-F., and Wittinghofer, A. (1989) *J. Mol. Biol. 205*, 269−273.
19. Watabe, S., Imai, J., Nakaya, M., Hirayama, Y., Okamoto, Y., Masaki, H., Uozumi, T., Hirono, I., and Aoki, T. (1995) *Biochem. Biophys. Res. Commun. 208*, 118−125.
20. Gornall, A. G., Bardawill, C. J., and David, M. M. (1949) *J. Biol. Chem. 177*, 751−765.
21. Laemmli, U. K. (1970) *Nature 227*, 680−685.
22. Matsudaira, P. (1987) *J. Biol. Chem. 262*, 10035−10038.
23. Bennet, P. M. (1981) *J. Mol. Biol. 146*, 201−221.
24. Yagi, N., and Offer, G. W. (1981) *J. Mol. Biol. 151*, 467−490.
25. Hirel, P.-H., Schmitter, J.-M., Dessen, P., Fayat, G., and Blanquet, S. (1989) *Proc. Natl. Acad. Sci. U.S.A. 86*, 8247−8251.
26. Lathrop, B. K., Burack, W. R., Biltonen, R. L., and Rule, G. S. (1992) *Protein Expression Purif. 3*, 512−517.
27. Atkinson, S. J., and Stewart, M. (1991) *J. Cell Sci. 99*, 823−836.
28. O'Halloran, T. J., Ravid, S., and Spudich, J. A. (1990) *J. Cell Biol. 110*, 63−70.
29. Yang, J. T., Wu, C.-S. C., and Martinez, H. M. (1986) *Methods Enzymol. 130*, 208−269.
30. Huxley, H. E (1963) *J. Mol. Biol. 7*, 281−308.
31. Kato, S., and Konno, K. (1993) *J. Biochem. (Tokyo) 113*, 43−47.
32. Watabe, S., Hwang, G.-C., Nakaya, M., Guo, X.-F., and Okamoto, Y. (1992) *J. Biochem. (Tokyo) 111*, 113−122.
33. Cohen, C., and Longley, W. (1966) *Science 152*, 794−796.
34. Cohen, C. Szent-Györgyi, A. G., and Kendrick-Jones, J. (1971) *J. Mol. Biol. 56*, 223−237.
35. Chaen, S., Nakaya, M., Guo, X.-F., and Watabe, S. (1996) *J. Biochem. (Tokyo) 120*, 788−791.
36. McLachlan, A. D., and Stewart, M. (1975) *J. Mol. Biol. 98*, 293−304.
37. McLachlan, A. D., Stewart, M., and Smillie, L. B. (1975) *J Mol. Biol. 98*, 281−291.
38. McLachlan, A. D., and Karn, J. (1982) *Nature 299*, 226−231.
39. Zhou, N. E., Kay, C. M., and Hodges, R. S. (1992) *Biochemistry 31*, 5739−5746.
40. Hwang, G.-C., Watabe, S., and Hashimoto, K. (1990) *J. Comp. Physiol. B 160*, 233−239.

BI972344G